Author/s:
Yan, Y;Gause, KT;Kamphuis, MMJ;Ang, CS;O'Brien-Simpson, NM;Lenzo, JC;Reynolds, EC;Nice, EC;Caruso, F

Title:
Differential roles of the protein corona in the cellular uptake of nanoporous polymer particles by monocyte and macrophage cell lines

Date:
2013-12-23

Citation:
Yan, Y., Gause, K. T., Kamphuis, M. M. J., Ang, C. S., O'Brien-Simpson, N. M., Lenzo, J. C., Reynolds, E. C., Nice, E. C. & Caruso, F. (2013). Differential roles of the protein corona in the cellular uptake of nanoporous polymer particles by monocyte and macrophage cell lines. ACS Nano, 7 (12), pp.10960-10970. https://doi.org/10.1021/nn404481f.

Persistent Link:
https://hdl.handle.net/11343/123282

Differential Roles of the Protein Corona in the Cellular Uptake of Nanoporous Polymer Particles by Monocyte and Macrophage Cell Lines

*Yan Yan,[‡] Katelyn T. Gause,[‡] Marloes M. J. Kamphuis,[‡] Ching-Seng Ang,[#] Neil M. O'Brien-Simpson,[+] Jason C. Lenzo,[+] Eric C. Reynolds,[+] Edouard C. Nice,[¶] and Frank Caruso[‡,]**

[‡]Department of Chemical and Biomolecular Engineering, The University of Melbourne, Parkville, Victoria 3010, Australia, [#]Bio21 Molecular Science and Biotechnology Institute, The University of Melbourne, Victoria 3010, Australia, [+]Melbourne Dental School, The University of Melbourne, Victoria 3010, Australia, [¶]Department of Biochemistry and Molecular Biology, Monash University, Victoria 3800, Australia

*AUTHOR EMAIL ADDRESS: fcaruso@unimelb.edu.au

ABSTRACT

Many biomolecules, mainly proteins, adsorb onto polymer particles to form a dynamic protein corona in biological environments. The protein corona can significantly influence particle-cell interactions, including internalization and pathway activation. In this work, we demonstrate the differential roles of a given protein corona formed in cell culture media in particle uptake by monocytes and macrophages. By exposing disulfide-stabilized poly(methacrylic acid) nanoporous polymer particles (PMA_{SH} NPPs) to complete cell growth media containing 10% fetal bovine serum (FBS), a protein corona, with the most abundant component being bovine serum albumin, was characterized. Upon the adsorption onto the PMA_{SH} NPPs, native bovine serum albumin (BSA) was found to undergo conformational changes. The denatured BSA led to a significant decrease in internalization efficiency in human monocytic cells, THP-1, compared with the bare particles, due to reduced cell membrane adhesion. By contrast, the unfolded BSA on the NPPs triggered class A scavenger receptor-mediated phagocytosis in differentiated macrophage-like cells (dTHP-1) without a significant impact on the overall internalization efficiency. Taken together, this work demonstrates the disparate effects of a given protein corona on particle-cell interactions, highlighting the correlation between protein corona conformation *in situ* and relevant biological characteristics for biological functionalities.

KEYWORDS: nanoporous polymer particles, protein corona, phagocytosis, monocytes, macrophage, class A scavenger receptors

The evaluation of complex interactions between particles and biological systems has become an active research endeavor in recent years, as such information is key to rationally designing particles for biological applications. Upon exposure to biological systems, particles are often vigorously recognized by front line immune cells, such as monocytes and macrophages. Monocytes, which are derived from bone marrow progenitors, circulate in the blood, and eventually emigrate into tissues where they differentiate into macrophages.[1] Macrophages are non-migratory, tissue-resident cells, which have high phagocytic ability to ingest pathogens and cellular debris.[2] The interactions between particles and monocyte-macrophages play a significant role in particle clearance, particle toxicity, and therapeutic efficacy.[3]

Many physicochemical properties of particles, such as size, shape and surface chemistry, have been shown to strongly influence their cellular interactions.[4] In biological fluids (*e.g.*, blood, plasma, interstitial fluid), proteins and other biomolecules adsorb onto particle surfaces to form a so called "protein corona". The formation of the protein corona gives rise to the biological identity of particles, which critically regulates their cell recognition and internalization.[5] Several studies have reported that the protein corona reduces the cell membrane adhesion of particles, leading to reduced cellular uptake.[6,7] In addition to the internalization kinetics, the protein corona has also been shown to influence the mechanisms of internalization.[8] For example, in the absence of serum, polystyrene nanoparticles are internalized by macrophages mainly *via* clathrin- and dynamin-dependent endocytosis. By contrast, in the presence of human serum, phagocytosis becomes the predominant internalization route of polystyrene nanoparticles.[8] Further, nanoparticles can induce structural changes of the adsorbed proteins,[9-11] which in turn play a significant role in cell signal transduction.[9] It has been shown that fibrinogen unfolding upon adsorption onto nanoparticles activates the NF-κB signal pathway *via* the integrin receptor, Mac-

1, to release inflammatory cytokines.[9] Clearly, the impact of a protein corona on particle interactions with cells is significant and diverse, as this phenomenon is strongly dependent on particle properties, the nature of the biological fluids, and cellular components. Therefore, to uncover underlying mechanisms associated with the biological identity of particles, there is a need to establish links between protein corona properties, cellular characteristics, and biological functions.

Template-based assembly has become a prominent approach for synthesizing polymer particles for biomedical applications because it combines control over particle morphology (*e.g.*, size and shape) with the versatility of polymer building blocks,[12,13] allowing tuning of the composition of the particles. Templating porous particles gives rise to a new class of free-standing polymer particles, namely nanoporous polymer particles (NPPs).[12,13] The assembly method to form NPPs involves infiltration of polymers into the internal space of porous templates, optional subsequent stabilization *via* covalent crosslinking, and template removal, resulting in the formation of polymer replica particles. Various NPPs with diverse composition, size, porosity and functionality have been synthesized by using mesoporous silica particles as templates.[12,13] Owing to the versatility, tunability and high cargo loading capacity, NPPs show promise for therapeutic delivery.[14-16] For example, nanoporous poly(L-glutamic acid) (PGA) microparticles have been used as carriers for sustainable delivery of brain-derived neurotrophic factor (BDNF) to rescue BDNF-deprived neuronal cells *in vivo*.[14] Additionally, nanoporous PGA particles loaded with CpG oligodeoxynucleotides have been shown to enhance immunogenicity as self-adjuvant particles *in vitro*.[15] NPPs have also been generated to address controlled drug delivery in cancer cells,[16] where the chemotherapeutic compound, doxorubicin (DOX), was conjugated to thiol-containing poly(methacrylic acid) (PMA_{SH}). The DOX-PMA_{SH} conjugates were infiltrated into

mesoporous silica particles and subsequently oxidized to form disulfide bonds between PMA_{SH}, resulting in DOX-loaded PMA_{SH} NPPs. It has been shown that the PMA_{SH} NPPs are internalized and transported to lysosomes in cancer cells,[17] and that the DOX-loaded PMA_{SH} NPPs exhibit significant cytotoxicity *in vitro*.[16] For the continued development of these NPPs for therapeutic delivery, studies that address the formation of protein corona on the NPPs and its interactions with immune cells are required. However, these investigations are yet to be performed.

Herein, we investigate the protein corona formed by exposing PMA_{SH} NPPs to cell culture media and evaluate its effect on cellular uptake in the monocytic THP-1 cells as well as differentiated macrophage-like THP-1 (dTHP-1). Although immortalized monocytic cell lines (*e.g.,* THP-1 or U937) have significant differences in gene expression compared with primary monocytes and macrophages, monocytic cell lines have been used as a model system in many studies *in vitro* due to their homogeneity and availability. Our proteomics data show that bovine serum albumin (BSA) is the major component of the protein corona formed on the NPPs following exposure to the cell growth media. The PMA_{SH} NPPs bind and induce unfolding of BSA. The resulting protein corona of the PMA_{SH} NPPs has been shown to exhibit distinctly different effects on cellular uptake in monocytes and macrophages. In the monocytic THP-1 cells, the adsorption of serum proteins or BSA alone on the particles decreases the particle-cell membrane adhesion, leading to reduced cellular uptake. By contrast, the identical protein coronas do not significantly change the overall internalization efficiency, but have an important impact on internalization mechanisms in dTHP-1 cells. Following the differentiation to macrophages, class A scavenger receptors (SR-A) that are present on the cell membrane recognize the unfolded BSA on the PMA_{SH} NPPs, leading to the activation of SR-A-mediated phagocytosis (Scheme 1). As serum albumin has been found to be present on most particle

surfaces upon exposure to plasma,[18] the current study highlights the significance of serum albumin conformation on particle-macrophage interactions, which has important implications in particle clearance. Taken together, our data provide important insights into the cellular uptake of PMA_{SH} NPPs in immune cells, showing that the biological interactions are determined by the combined properties of protein corona and cellular components.

RESULTS AND DISCUSSION

PMA_{SH} NPPs with a diameter of approximately 500 nm were synthesized as described previously,[16] and incubated with complete cell growth media containing 10% fetal bovine serum (FBS) to form the protein corona. The resulting PMA_{SH} NPP-serum protein complexes were separated from the media by centrifugation and washed with Dulbecco's Phosphate-Buffered Saline (DPBS) extensively to remove unbound proteins. These long-lived proteins, namely the hard protein corona, were subsequently eluted, separated by sodium dodecyl sulfate polyacrylamide gel electrophoresis (SDS-PAGE), and stained with Coomassie G-250. It was shown that the hard protein corona was comprised of a number of serum proteins with a predominant band of ~70 kDa (Figure 1a). The formation of the protein corona is a rapid process, as exposure to the cell growth media for 5 min results in significant protein adsorption, as shown by SDS-PAGE (Figure 1a). The rapid formation of the protein corona upon exposure to human plasma has also been reported for silica and polystyrene nanoparticles.[19]

To identify the composition of the protein corona after 1 h of incubation with complete cell growth media containing 10% FBS, the corresponding lane from the SDS-PAGE (lane 5 in Figure 1a) was excised into 13 equal fractions followed by in-gel tryptic digestion and protein identification using an Orbitrap Elite mass spectrometer (Thermo Scientific). The major band at

~70 kDa was used to align the gel for excision of the bands. A total of 154 proteins were identified from the protein corona based on a targeted 1% false discovery rate and a minimum of 2 unique peptides (Table S1). Exponentially modified protein abundance index (emPAI) was used to estimate the relative concentration of proteins in the sample, as reported previously.[20] BSA was found to have the highest emPAI (348) and mol % (43) of all identified proteins with a total sequence coverage of ~80% and 63 unique peptides identified. The next most abundant protein, with an emPAI score of 179.23 was fetal hemoglobin subunit beta. We further performed a localized analysis on the most intensely stained band at ~70 kDa. In agreement with overall protein abundance, BSA was also identified as the major protein in this band with 73.5% sequence coverage, 55 unique peptides and an emPAI score of 168 (Table S2). Alpha-fetoprotein ranked second with an emPAI score of 2.59.

To quantify the amount of BSA adsorbed on the NPPs, densitometry analysis on BSA stained with Coomassie G-250 was performed. The protein corona from known amounts of both NPPs and BSA (as standards for densitometry analysis) were loaded onto the same SDS-PAGE gel and stained with Coomassie G-250. Densitometry analysis of the BSA bands using Quantify One 1-D Analysis Software (Bio-Rad) revealed that 1×10^8 PMA_{SH} NPPs adsorbed about 900 ng BSA from the cell growth media (Figure S1). This corresponds to 9×10^{-15} g of BSA adsorbed per NPP.

To evaluate the effect of the protein corona on particle size and surface charge, the NPPs were dispersed in three types of media for comparison, namely serum-free RPMI medium (SF), complete RPMI medium containing 10% heat-inactivated FBS (cRPMI), and RPMI medium containing 2 mg mL^{-1} BSA (approximately equivalent to BSA concentration in cRPMI[21]) (BSA). Particle size and zeta-potential analysis of these three different particle-medium dispersions were

undertaken using dynamic light scattering and microelectrophoresis, respectively. In comparison to SF medium, the particle size distribution shifted to higher values for both cRPMI and BSA media as a result of protein adsorption (Figure 1b). An increase in particle size due to the formation of a protein corona has been commonly observed in other particles, such as polystyrene and silica nanoparticles.[22] It is also noted that the increase of hydrodynamic diameter measured by DLS cannot be necessarily quantitatively related to the thickness of the protein layer, as the apparent size distribution is generally broadened when multiple species are present.[23] The zeta-potential of the NPPs was also altered upon protein adsorption, from -39 ± 5 mV in SF medium to -25 ± 4 mV and -26 ± 5 mV in the cRPMI and BSA media, respectively. Studies have reported that the adsorption of proteins leads to a neutralization in particle surface charge both in positively charged[24] and negatively charged nanoparticles,[22] presumably by binding to proteins with opposite charge. However, significant electrostatic binding between the PMA_{SH} NPPs and BSA is not expected because both BSA (pI = 4.7) and the NPPs are negatively charged in these media at pH 7.4. This suggests that other interactions, such as hydrophobic interactions, may play a role in the formation of protein corona.[5,10] A recent study has shown that the strong binding observed when negatively charged fibrinogen binds with negatively charged poly(acrylic acid)-conjugated gold nanoparticles is due to the exposure of a positively charged domain in fibrinogen induced by adsorption onto the nanoparticles.[9] Therefore, we sought to examine whether conformational changes in BSA occur upon binding to the PMA_{SH} NPPs. To monitor the protein secondary structure, far-ultraviolet circular dichroism (CD) was employed. The typical native BSA CD spectrum with α-helix and β-sheet structures was observed when native BSA is dissolved in DPBS (0.3 mg mL^{-1}) (Figure 2). By contrast, the PMA_{SH} NPPs exhibited basal ellipticity. However, the BSA CD spectra progressively shifted to higher

ellipticity values from 205 nm to 225 nm in the presence of increasing concentrations of the PMA_{SH} NPPs, suggesting that conformational changes of BSA occur in the presence of the NPPs (Figure 2). Generally, the α-helix has negative ellipticity at 222 nm and 208 nm, whereas the β-sheet shows a negative band at 218 nm. Our data indicate that there were minor structural perturbations of BSA, probably both on the α-helix and β-sheet, upon adsorption onto the NPPs. Similar effects have been seen with gold nanoparticles.[25] Protein adsorption onto particles is a kinetic process and is influenced by a number of parameters, including protein concentration and particle size. Lower protein concentration can lead to lower surface coverage, which in turn may favor surface-induced conformational changes of proteins.[26,27] Hence, it is noted that the BSA conformation change upon adsorption onto the NPPs can vary between different serum mixtures.

Next, we investigated the effects of the protein corona on cellular uptake of the PMA_{SH} NPPs in monocytic THP-1 and macrophage-like dTHP-1 cells. The PMA_{SH} NPPs were fluorescently labeled with Alexa Fluor 633 (AF633), and the resulting AF633-PMA_{SH} NPPs were counted using flow cytometry. Both THP-1 and dTHP-1 cells were incubated in the three types of media (SF, cRPMI, and BSA) with the AF633-PMA_{SH} NPPs at a particle-to-cell ratio of 100:1 for various time intervals. The percentage of cells associated (including surface bound and internalized) with the NPPs was evaluated by flow cytometry.

In the case of THP-1 cells, the presence of a protein corona showed a significant effect on the cellular association. It was shown that in both cRPMI and BSA media, the cellular association only increased fractionally from 1 h (28%) to 6 h (37%), suggesting slow cell binding and internalization. By contrast, the cellular association was shown to be significantly higher (> 2-fold) in SF medium at all time intervals over the 6 h incubation (Figure 3a). To confirm that the formation of the protein corona was directly related to the reduced cellular association, the

PMA_{SH} NPPs were preincubated with the cRPMI to allow the protein to adsorb onto the particle surface. Subsequently, the coated NPPs were added to the THP-1 cells in the SF medium. It was shown that the cellular association was significantly inhibited compared with the uncoated PMA_{SH} NPPs, in particular, at the 1 h and 3 h time points (Figure S2). The gradual decrease in difference in cellular association between coated and uncoated NPPs is possibly due to the disassociation of the protein corona from the NPPs in the serum free medium. Consistently, the reduced internalization of the PMA_{SH} NPPs in both cRPMI and BSA media at 6 h was confirmed by deconvolution fluorescence microscopy (Figure 3b, c and d, Figure S3). This observation is in good agreement with other studies that show decreased cellular uptake of polystyrene,[8] silica,[6] and gold nanoparticles,[24] to various extents, due to the presence of serum proteins. The internalization of particles generally follows a multistep process involving initial cell surface contact, cell membrane adhesion, and subsequent internalization *via* energy-dependent endocytosis. Hence, we next examined the membrane adhesion properties of the PMA_{SH} NPPs in the three types of media to further uncover the role of the protein corona in cellular uptake. The PMA_{SH} NPPs were incubated with THP-1 cells at the same dose at 4 ºC for 30 min to allow particle adhesion to the cell membrane without internalization. After incubation, the cells were washed with DPBS to remove the unbound NPPs, and subsequently incubated in particle-free cRPMI medium at 37 ºC for 3 h to allow internalization of the surface-bound NPPs. Using this approach, reproducible quantification of particle adhesion to the cell membrane can be obtained.[7] Using flow cytometry, the percentage of cells with internalized NPPs was measured. A significantly higher percentage of cells with NPPs (about 3-fold) was observed for the treatment in SF medium compared with cRPMI and BSA media (Figure 4), indicating reduced cell membrane adhesion of particles due to the formation of protein coronas. Clearly, the reduced cell

membrane adhesion of the NPPs in the presence of the protein coronas leads to the decreased cellular uptake. This finding is consistent with other studies, where nonspecific binding of nanoparticles are reduced by protein adsorption, resulting in slower and overall reduced nanoparticle uptake.[6,7,24,28] Interestingly, the cellular association kinetics and cell membrane binding of the NPPs in the BSA medium were found to be similar to those in the cRPMI medium, suggesting that BSA, as the major component in the serum protein corona, plays a dominant role in the functionality of the serum protein corona in relation to THP-1 cell recognition. These results show that the formation of the protein-NPP complex inhibits cellular binding, resulting in decreased cellular internalization in monocytic THP-1 cells.

Next, the cellular association and uptake of the AF633-PMA_{SH} NPPs in macrophage-like dTHP-1 cells were investigated. To induce macrophage-like differentiation in monocytic THP-1 cells, a protocol reported previously using phorbol 12-myristate 13-acetate (TPA) was applied.[8, 29-31] TPA treatment, which activates protein kinase C (PKC), results in increased cell adherence, phagocytosis capability, and expression of surface macrophage markers.[30] Studies have shown that THP-1 derived macrophages (dTHP-1) overexpress SR-A, whereas monocytes exhibit very low levels of SR-A expression.[8,32] SR-A are a family of cell surface pattern recognition receptors that are able to bind multiple ligands,[33] including modified lipoproteins (*e.g.*, acetylated low-density lipoproteins, AcLDLs), modified proteins (*e.g.*, methylated BSA, mBSA), and polyanionic ligands (*e.g.*, oligonucleotide-functionalized gold nanoparticles[28]). Unlike THP-1 cells, the three different media did not dramatically influence the cellular association kinetics of the PMA_{SH} NPPs with dTHP-1 cells (Figure 5). The most pronounced difference among the treatment media was observed at 1 h with about 60% of cells associated with NPPs in the cRPMI or BSA media and 40% in the SF medium (Figure 5). The effective internalization of the NPPs

in the three types of media by dTHP-1 cells after 3 h incubation was further confirmed by deconvolution fluorescence microscopy (Figure 5). This result suggests that the protein corona plays a different role in the interactions with dTHP-1 cells compared with THP-1, which is most likely due to the presence of phagocytosis receptors at the cell surface after differentiation. Given the polyanionic nature of the NPP-protein complex and increased cell surface expression of SR-A, we sought to probe the link between the protein corona and SR-A. A SR-A inhibitory ligand, polyinosinic acid (poly I), was used to block SR-A-mediated phagocytosis. In parallel, a chemically related compound that does not interact with SR-A, polycytidylic acid (poly C), was used as a negative control. The cells were preincubated in either SF, cRPMI, or BSA media with the inhibitory ligand or control for 30 min prior to the addition of the PMA_{SH} NPPs. It was shown that poly I significantly attenuated the NPP-cell association in both cRPMI and BSA media to similar extents, while poly C had no effect (Figure 5). By contrast, poly I did not affect the NPP-cell association in the SF media, suggesting SR-A-mediated phagocytosis is not operational in the absence of the protein corona. In addition, it was found that the poly I and poly C treatments did not affect the uptake of the NPPs in THP-1 cells (Figure S4), which is consistent with the fact that THP-1 cells have negligible level of SR-A expression.[8] The inhibition of the NPP uptake by poly I in the cRPMI and BSA media was also confirmed using deconvolution fluorescence microscopy (Figure 5). After incubation for 3 h in the presence or absence of poly I, the cell membrane was stained with wheat agglutinin (green, Figure 5). A significant decrease in the number of PMA_{SH} NPP internalized by dTHP-1 cells was observed in the presence of poly I (Figure 5). These data suggest that the serum protein-PMA_{SH} and BSA-PMA_{SH} NPP complexes are recognized by SR-A, whereas the bare PMA_{SH} NPPs do not bind to SR-A. Since native BSA is not a ligand of SR-A,[34] a likely reason for the unexpected affinity to

SR-A could be the unfolding of BSA on the NPPs. It has been shown that SR-A binds to many denatured or modified endogenous proteins, such as denatured collagen type I and β-amyloid fibrils, to mediate their clearance.[35,36] It has been shown that a collagen-like domain containing a lysine cluster in SR-A, which forms a positively charged groove, is a key site for ligand binding.[36] In general, the SR-A ligands are polyanionic macromolecules, as they specifically interact with positively charged binding domains. Changes in the BSA overall structure upon adsorption on the PMA_{SH} NPPs may lead to the exposure of negatively charged amino acid residues of BSA, which trigger interactions with SR-A. Combined, these results show that the adsorption of serum proteins or BSA on the PMA_{SH} NPPS does not significantly impact the total uptake of the NPPs in dTHP-1 cells. More importantly, the formation of the protein corona provides the biological identity for the PMA_{SH} NPPs and allows different internalization mechanisms compared with the bare NPPs by promoting SR-A-mediated phagocytosis.

To investigate cytokine secretion induced by the serum protein-PMA_{SH} NPP complexes, both THP-1 and dTHP-1 cells were treated with PMA_{SH} NPPs with an increasing particle-to-cell ratio (0, 1, 10, 100, and 1000) in cRPMI medium for 24 h. Subsequently, the respective supernatants were collected, and the levels of cytokines and nitric oxide (NO) induced were determined. The PMA_{SH} NPPs did not induce the secretion of NO in THP-1 or dTHP-1 cells at any of the particle-to-cell ratios examined (Figure S5), indicating that the PMA_{SH} NPPs do not activate the NF-κB signaling pathway *via* Toll-like receptors (TLRs). By using a multiplex microbead array assay, the secretion of 27 cytokines was evaluated. Significant changes in cytokine induction were only observed in dTHP-1 cells (Figure 6). It was shown that the PMA_{SH} NPPs induced a significant ($p < 0.05$) but small increase in 11 cytokines: interleukin (IL)-1β, IL-2, IL-6, IL-8, IL-9, IL-17A, eotaxin, interferon (IFN)-γ, macrophage inflammatory protein (MIP)-1α, MIP-1β, and

tumor necrosis factor (TNF)-α in dTHP-1 cells only at a 1000:1 particle-to-cell ratio (Figure 6). Of these IL-1β, IL-2, IL-8, MIP-1α, MIP-1β and TNF-α were increased 2-4 fold above background levels. IL-5 and IL-7 were not detected (data not shown) in our assay. IL-1ra, IL-10, IL-12p70, IL-13, IL-15, basic fibroblast growth factor (Basic FGF), granulocyte colony stimulating factor (G-CSF), granulocyte-macrophage colony stimulating factor (GM-CSF), interferon gamma-induced protein-10 (IP-10), monocyte chemoattractant protein-1 (MCP-1), platelet-derived growth factor-BB (PDGF-BB), regulated on activation, normal T cell expressed and secreted (RANTES) and vascular endothelial growth factor (VEGF) were all expressed without a significant change upon the exposure to the NPPs (Figure S6). Moreover, using YO-PRO-1 as a measure of early apoptosis and the nucleic acid dye propidium iodide (PI) as an indicator of cell death, it was shown that PMA_{SH} NPPs did not induce cell death/necrosis in THP-1 or dTHP-1 cells at any of the particle-to-cell ratios tested (Figure S7). No indication of apoptosis was found in THP-1 cells and only a 10% increase in early apoptosis (YO-PRO-1+ cells) above background was observed in the dTHP-1 cells at a 1000:1 ratio (Figure S7).

Taken together, the low level of pro-inflammatory cytokine secretion, no production of NO, and low level early apoptosis[37,38] observed in dTHP-1 cells are in good agreement with the notion that SR-A mediated phagocytosis is involved in the internalization of PMA_{SH} NPPs in the presence of serum proteins.

CONCLUSIONS

The present study provides the first detailed investigation on the protein corona of NPPs formed in cell growth medium and its impacts on the cellular uptake in both monocytes and macrophages. Our data show that many serum proteins adsorb onto the PMA_{SH} NPPs upon

exposure to cell growth medium, and BSA is the most abundant protein in the resulting protein corona. Importantly, BSA undergoes conformational changes as a result of adsorption onto the negatively charged PMA_{SH} NPPs, leading to distinctively different biological functions in monocytes and macrophages. In the monocytic THP-1 cells, the adsorption of BSA onto the NPPs reduces the particle-membrane adhesion, resulting in significantly lower internalization efficiency. By contrast, in the macrophage-like dTHP-1 cells, the expression of SR-A on the cell surface, following TPA-induced differentiation, activates a particle-cell recognition mechanism that is unique to the protein-PMA_{SH} NPP complexes compared with the bare PMA_{SH} NPPs. Due to the structural perturbation of BSA on the PMA_{SH} NPPs, SR-A, which bind to many denatured forms of proteins, recognize the BSA-PMA_{SH} NPP complexes and trigger activation of the SR-A-mediated phagocytosis. While several studies have reported decreased particle internalization as a result of serum protein adsorption, this study demonstrates both a similar (in THP-1 cells) and an alternative (in dTHP-1 cells) effect of a given protein corona on cellular uptake, highlighting the need to critically correlate protein corona functionality with specific biological traits. Our data also underscores the importance of the conformation of the protein corona in cell recognition. This suggests that understanding both the composition and orientation of the protein corona is important for evaluation of its biological interaction. In addition, the size of the NPPs, including the heterogeneity of the particles, may also influence the formation of the protein corona, which can further impact cellular uptake kinetics and the mechanisms of action. To develop PMA_{SH} NPPs for biological applications, future studies will be aimed at modulating the PMA_{SH} NPP properties (*e.g.*, surface chemistry and porosity) to control the formation of the protein corona and their biological ramifications. Given the critical role of SR-A in innate

immunity and inflammatory diseases, this study provides important insights into the biological responses of PMA_{SH} NPPs.

METHODS

Materials: Poly(methacrylic acid, sodium salt) (PMA, M_w 15 kDa) was purchased from Polysciences (USA). *N*-chloro-p-toluenesulfonamide sodium salt (chloramine T), hydrofluoric acid (HF), dithiothreitol (DTT), sodium citrate dihydrate, 1-pentanol tetraethyl orthosilicate (TEOS), N-(3-dimethylaminopropyl)-N′-ethylcarbodiimide hydrochloride (EDC), (3-aminopropyl)-triethoxysilane (APTES), iodoacetamide, bovine serum albumin (BSA), polyinosinic acid (poly(I)), polycytidylic acid (poly(C)), and phorbol 12-myristate 13-acetate (TPA) were purchased from Sigma-Aldrich and used as received. 3-(*N*-morpholino)propanesulfonic acid (MOPS) was obtained from Acros Organics. Sodium acetate (NaOAc), 2-(*N*-morpholine)-ethane sulfonic acid (MES), and ammonia were purchased from Merck. Pyridine dithioethylamine hydrochloride (PDA-HCl) was obtained from Shanghai Speed Chemical Co. Ltd., China. 4% paraformaldehyde was purchased from Electron Microscopy Sciences, USA. Alexa Fluor® 633 hydrazide (AF633) reactive dyes, Roswell Park Memorial Institute 1640 containing GlutaMax (RPMI), heat-inactivated fetal bovine serum (HI-FBS), Dulbecco's Phosphate-Buffered Saline (DPBS), NuPAGE Bis-Tris Precast Gel 4-12%, NuPAGE MES SDS Running Buffer, NuPAGE LDS Sample Buffer, NuPAGE Sample Reducing Agent, and AF488-Wheat germ agglutinin were purchased from Life Technologies. Ultrapure water with resistance greater than 18 MΩ cm was obtained from an inline Millipore RiOs/Origin system (Millipore Corporation, USA).

Preparation of PMA_{SH} NPPs: PMA_{SH} NPPs were prepared as described previously.[17] Briefly, approximately 5 mg mL^{-1} APTES-modified MS particles were dispersed in 5 mg mL^{-1} of PMA_{SH} solution in NaOAc buffer (50 mM, pH 4.5) overnight to allow the infiltration of polymer to the internal porous network. After incubation, the excess polymer was removed by

centrifugation, and particles were washed with NaOAc buffer. The particles were then dispersed in NaOAc buffer and crosslinked by NaOAc buffer (pH 6, 50 mM) containing chloramine T (10 mM) for 2 min. Afterwards, the particles were washed with PBS buffer, and the MS templates were dissolved with a 2 M HF/8 M NH_4F solution (pH ~5). *Caution! HF is highly toxic. Extreme care should be taken when handling HF solution and only small quantities should be prepared*. The resulting PMA_{SH} NPPs were washed with Milli-Q water three times and labeled with hydrazide-AF633 in DPBS buffer. The AF633-labeled PMA_{SH} NPPs were counted using a CyFlow Space (Partec GmbH) flow cytometer with 488 nm and 633 nm lasers, and the concentration was determined based on the absolute volume of the flow cytometer.

Protein Corona on PMA_{SH} Particles: PMA_{SH} particles were incubated with RPMI media containing 10% (v/v) HI-FBS at room temperature (RT, 25 ºC) for 5 min, 15 min, 30 min, 1 h or 2 h. The particles were collected by centrifugation at 5000 *g* for 5 min and washed three times with DPBS. The proteins adsorbed on the particles were eluted with NuPAGE LDS Sample Buffer at 70 °C for 10 min, and reduced by NuPAGE Sample Reducing Agent at 70 °C for 10 min. The proteins were then separated on NuPAGE Bis-Tris Precast Gel 4-12% by gel electrophoresis. The gel was stained with Coomassie G-250 (SimplyBlue SafeStain, Invitrogen).

In-Gel Tryptic Digestion: Gel bands were excised manually from the gel with a scalpel and destained with a solution of 50 mM ammonium bicarbonate and 50% acetonitrile. Proteins were then reduced in 2.5 mM DTT at 60 °C for 30 min, followed by alkylation with 10 mM iodoacetamide for 30 min in the dark at RT. The gel pieces were washed and dehydrated with alternating wash cycles of 50 mM ammonium bicarbonate and acetonitrile. After complete dehydration of the gel slice, it was rehydrated with a solution containing 0.5 μg trypsin (Promega corp., Madison, WI, USA) in 20 mM ammonium bicarbonate. The gel pieces were incubated at

37 °C overnight followed by acidification with formic acid (1% v/v) before loading onto the mass spectrometer.

Mass Spectrometry Analysis: Tryptic digests were analyzed by LC-MS/MS using a LTQ Orbitrap Elite (Thermo Scientific) with a nanoelectrospray interface coupled to an Ultimate 3000 RSLC nanosystem (Dionex). The nanoLC system was equipped with an Acclaim Pepmap nano-trap column (Dionex – C18, 100 Å, 75 µm × 2 cm) and an Acclaim Pepmap analytical column (Dionex C18, 2µm, 100 Å, 75 µm × 15 cm). 2 µL of the peptide mix was loaded onto the trap column at an isocratic flow of 4 µL min^{-1} of 3% CH_3CN containing 0.1% formic acid for 5 min before the enrichment column was switched in-line with the analytical column. The eluents used for the liquid chromatography were 0.1% (v/v) formic acid (solvent A) and 100% CH_3CN/0.1% formic acid (v/v). The following gradient was used: 3% to 12% B for 1 min, 12% to 35% B for 20 min, 35% to 80% B for 2 min and maintained at 80% B for 2 min followed by equilibration at 3% B for 7 min before the next sample injection. The LTQ Orbitrap Elite mass spectrometer was operated in the data dependent mode with nano ESI spray voltage of +2.0 kv, capillary temperature of 250 ^{o}C and S-lens RF value of 60%. Spectra were acquired first in positive mode with full scan, scanning from m/z 300-1650 in the FT mode at 240 000 resolution followed by collision-induced dissociation (CID) in the linear ion trap with the ten most intense peptide ions with charge states ≥2 isolated and fragmented using normalized collision energy of 35 and activation Q of 0.25. Data were analyzed using Proteome Discoverer (Thermo Scientific version 1.4) with Mascot (Matrix Science version 2.4) against the Uniprot database. Search parameters were: precursor mass tolerance of 20 ppm, fragment mass tolerance of 0.8 Da, carbamidomethyl of cysteine as fixed modification, and oxidation of methionine as variable modifications. Trypsin with a maximum of two missed cleavages was used as the cleavage enzyme. Search results were

set to a maximum of 1% false discovery rate (FDR) with two unique peptides required for positive identification. The relative concentration of proteins in the sample was estimated using the exponentially modified protein abundance index (emPAI).[20] To normalize for emPAI difference between runs, the protein content (mol %) of individual proteins in the sample was then calculated by dividing the individual emPAI values by the sum of all emPAI values within the sample and then multiplying it by 100.[20]

Dynamic Light Scattering and Zeta Potential Measurements: Particle sizes and zeta-potential were measured using a Malvern Zetasizer Nano ZS (Worcestershire, UK) at 25 ºC in three different solutions. Particle size measurements by dynamic light scattering (DLS) were carried out in RPMI medium, RPMI medium containing 10% HI-FBS (cRPMI), and RPMI medium containing 2 mg mL^{-1} BSA (BSA) solutions. Zeta-potential measurements were carried out in 10 × diluted RPMI, cRPMI, and BSA solutions to avoid a high concentration of salts.

Circular Dichroism Spectroscopy: Circular dichroism (CD) spectra were recorded using a model 410 circular dichroism spectrometer (Aviv Biomedical, Inc.) at 25 ºC. BSA solution (0.3 mg mL^{-1} in DPBS) was transferred to the CD cuvette after incubation with a different number of PMA_{SH} particles at 25 ºC for 60 min. Data were collected every 0.5 nm over the range of 190−250 nm.

Cell Culture: Human monocytic leukemia cell line THP-1 (American Type Culture Collection) cells were maintained in RPMI media with the addition of 10% (v/v) HI-FBS at 37 °C in a 5% CO_2 humidified atmosphere. Macrophage-like THP-1 (dTHP-1) were differentiated from THP-1 cells by the treatment with 200 nM TPA for 48 h in the complete growth media.

Cellular Association of PMA_{SH} Particles by Flow Cytometry: The cellular association was quantified as described previously.[39] THP-1 or dTHP-1 cells were incubated with particles at

a density of 1×10^5 cells in 0.5 mL media containing 1×10^7 AF633-PMA_{SH} particles in 24-well plates at 37 °C, 5% CO_2. After treatment for different time intervals, cells were then collected and washed with DPBS three times with centrifugation at 300 *g* for 5 min between washes. The cell pellet was resuspended in DPBS and analyzed by flow cytometry (CyFlow Space, Partec GmbH). At least 10 000 cells were analyzed for each treatment. The data were presented as a percentage of cells associated with the particles.

Cellular Uptake of PMA_{SH} Particles by Fluorescence Deconvolution Microscopy: THP-1 or dTHP-1 cells were treated with AF633-PMA_{SH} particles at a particle-to cell ratio of 100:1. The cells were then washed with DPBS three times to remove excessive particles and fixed with 4% paraformaldehyde for 20 min at RT. The cell membrane was stained with AF488-Wheat germ agglutinin (5 μg mL^{-1}) in DPBS at RT for 10 min. Optical sections of cell images were collected using a fluorescence deconvolution microscope (Delta Vision, Applied Precision). Images were processed with Imaris 6.3.1 software (Bitplane) and presented in maximum intensity projection.

Cell Membrane Adhesion of PMA_{SH} Particles by Flow Cytometry: THP-1 cells were incubated with particles at a density of 1×10^5 cells in 0.5 mL media containing 1×10^7 AF633-PMA_{SH} particles in 24-well plates at 4 °C for 30 min. The cells were then washed with DPBS twice with centrifugation at 300 *g* for 5 min between washes to remove excess particles. The cells were further incubated in the particle-free complete growth media at 37 °C, 5% CO_2 for 3 h to allow internalization of the cell surface-bound particles. The cells were trypsinized, collected by centrifugation at 300 *g* for 5 min, resuspended in DPBS, and analyzed by flow cytometry (CyFlow Space, Partec GmbH). At least 10 000 cells were analyzed for each treatment. The data were presented as a percentage of cells associated with the particles.

Inhibition of Scavenger Receptor A-Mediated Phagocytosis: Macrophage-like THP-1 cells (dTHP-1) were differentiated from monocytic THP-1 cells at a density of 1×10^5 cells in 0.5 mL complete growth media containing with 200 nM TPA for 48 h. After the differentiation, dTHP-1 cells were pretreated with poly(I), an inhibitor of scavenger receptor A, or poly(C), as control, for 30 min. The cells were further incubated with 1×10^7 AF633-PMA_{SH} particles in the presence or absence of poly(I) or poly(C) for various time intervals. Cellular association with particles was then performed and analyzed as described above.

Cytokine Assay: NPPs were added to THP-1 or dTHP-1 cells at increasing ratios and incubated for 24 h at 37 ^{o}C, 5% CO_2 in cRPMI. For THP-1 cells, the supernatant was collected by centrifugation at 800 *g* for 5 min to remove cells and then 17 000 *g* for 5 min to remove any remaining particles. For dTHP-1 cells, the supernatant was collected from the adherent cells and then centrifuged at 17 000 *g* for 5 min to remove any remaining particles. Cytokine levels in the supernatant were measured using a Bio-Plex Pro Human Cytokine Standard 27-Plex, Group 1 kit (Bio-Rad) on a Bio-Plex 200 System (Bio-Rad) as per the manufacturer's instructions.

ACKNOWLEDGMENT

This work was supported by the Australian Research Council under the Australian Laureate Fellowship (F.C., FL120100030) and Discovery Early Career Researcher Award (Y.Y., DE130100488), and by the National Health and Medical Research Council (NHMRC) Program Grant 487922 (F.C.). The authors gratefully acknowledge Dr Jiwei Cui (The University of Melbourne) for assistance with the particle synthesis, Ms Shane Reeve (Monash Biomedical

Proteomics Facility, Monash University, Clayton) for the initial mass spectrometry analysis on the HCT ULTRA ion trap mass spectrometer.

Supporting Information Available: Methods for the quantification of the BSA in the protein corona, apoptosis assay, and nitric oxide determination. Table of the protein composition in the protein corona, table of the protein composition of the major band on the SDS-PAGE, SDS-PAGE for BSA quantification, cellular association of protein-coated PMA_{SH} NPPs in THP-1 cells in serum free medium, fluorescence images (single z-plane) of uptake of the NPPs in THP-1 cells, cellular uptake of the NPPs in the presence of SR-A inhibitors in THP-1 cells, nitric oxide production by THP-1 and dTHP-1 cells, cytokine secretion by THP-1 and dTHP-1 cells, and early apoptosis and cell death assay of THP-1 and dTHP-1 cells. This material is available free of charge *via* the Internet at http://pubs.acs.org.

AUTHOR INFORMATION

Corresponding Authors

*Address correspondence to fcaruso@unimelb.edu.au

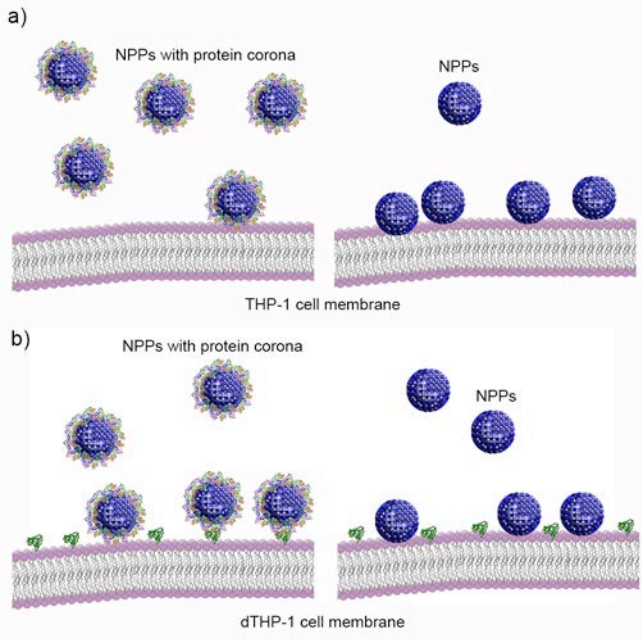

Scheme 1. a) In the THP-1 cells, the formation of the protein corona decreases the particle-cell membrane adhesion, leading to reduced cellular uptake. b) In the dTHP-1 cells with the expression of class A scavenger receptors (SR-A) on the cell membrane, the adsorption of proteins on the NPPs activates SR-A-mediated phagocytosis.

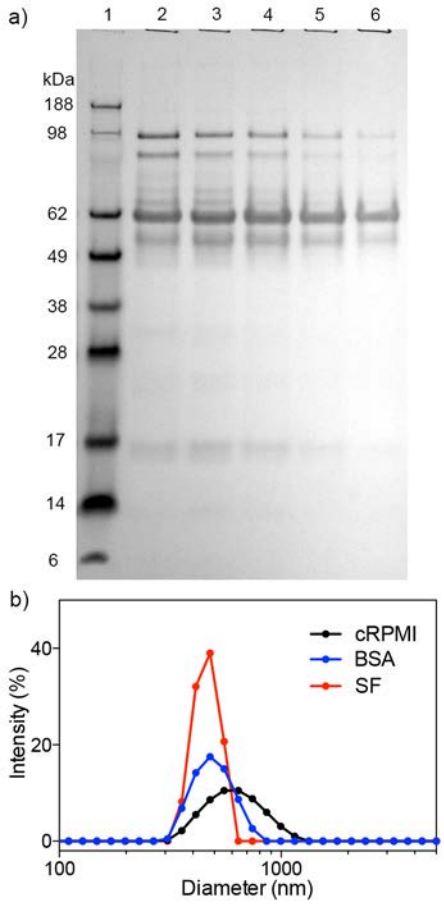

Figure 1. a) SDS-PAGE of protein coronas recovered from PMA_{SH} NPPs following incubation with cRPMI for various time periods (lane 2: 5 min, lane 3: 15 min, lane 4: 30 min, lane 5: 1 h, and lane 6: 2 h) at room temperature (25 °C). b) Size distribution of PMA_{SH} particles measured by DLS in different dispersants. cRPMI: RPMI medium containing 10% FBS, BSA: RPMI medium containing 2 mg mL^{-1} BSA, SF: serum-free RPMI medium.

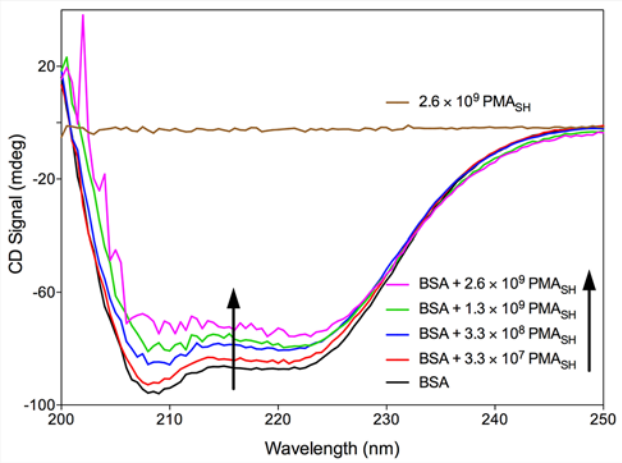

Figure 2. Circular dichroism spectra of BSA in the absence and presence of increasing concentrations of PMA_{SH} particles. BSA (0.3 mg mL^{-1}) solution was incubated with various concentrations of PMA_{SH} particles (indicated inset) at 25 °C for 60 min. The particles alone at the highest concentration showed a baseline CD signal.

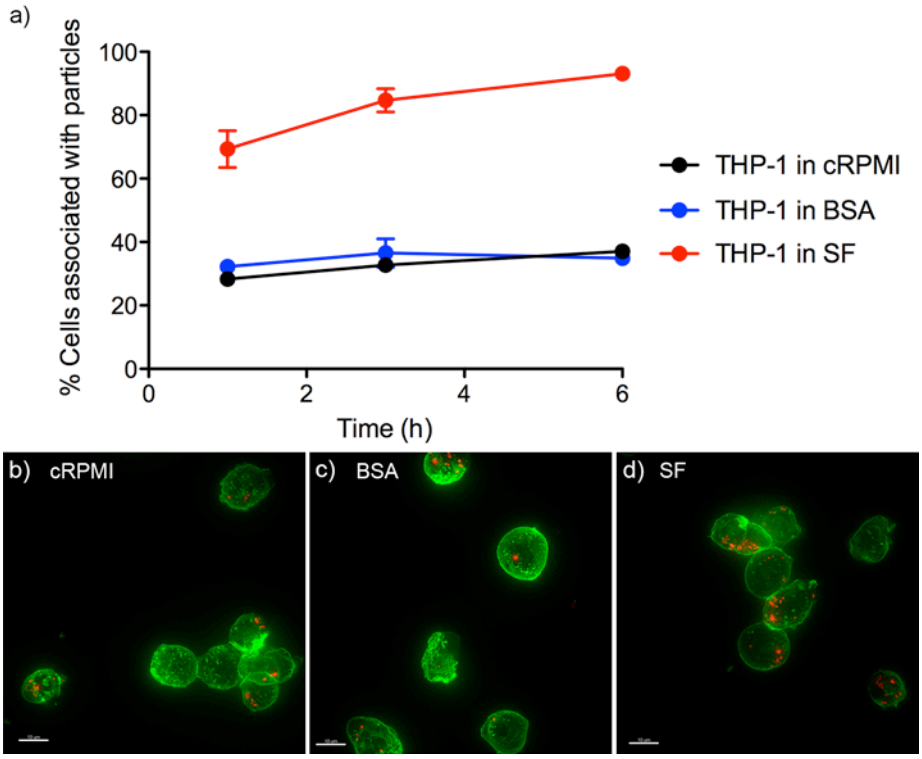

Figure 3. a) Cellular association of AF633-PMA_{SH} particles in THP-1 in complete growth medium (cRPMI), BSA-containing medium (BSA), or serum free medium (SF). Cells were incubated with the particles at a particle-to-cell ratio of 100:1 at 37 °C, 5% CO_2. The percentage of cells associated with particles was measured by flow cytometry. Data are the mean ± standard error of three independent experiments, and at least 10 000 cells were analyzed in each experiment. Cellular uptake of the particles in cRPMI (b), BSA (c), or SF (d) at 37 °C, 5% CO_2 for 6 h was visualized by fluorescence deconvolution microscopy. The maximum intensity projection images show the cell membrane (stained with AF488-wheat germ agglutinin, green) and internalized AF633-PMA_{SH} particles (Red). Scale bars = 10 μm.

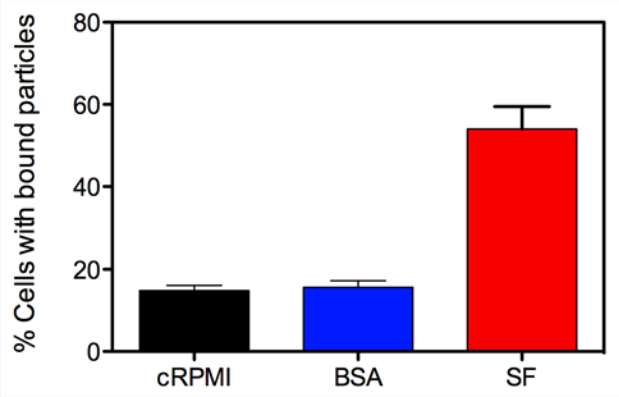

Figure 4. Cell surface binding of AF633-PMA_{SH} particles to THP-1 cells. Cells were incubated with particles in complete growth medium (cRPMI), BSA-containing medium (BSA), or serum free medium (SF) at 4 °C for 30 min, followed by washing with DPBS to remove excess unbound particles. Cells were further incubated in complete growth media at 37 °C, 5% CO_2 for 3 h to allow internalization of the surface-bound particles. The percentage of cells associated with particles was measured by flow cytometry. Data are the mean ± standard error of two independent experiments, and at least 10 000 cells were analyzed in each experiment.

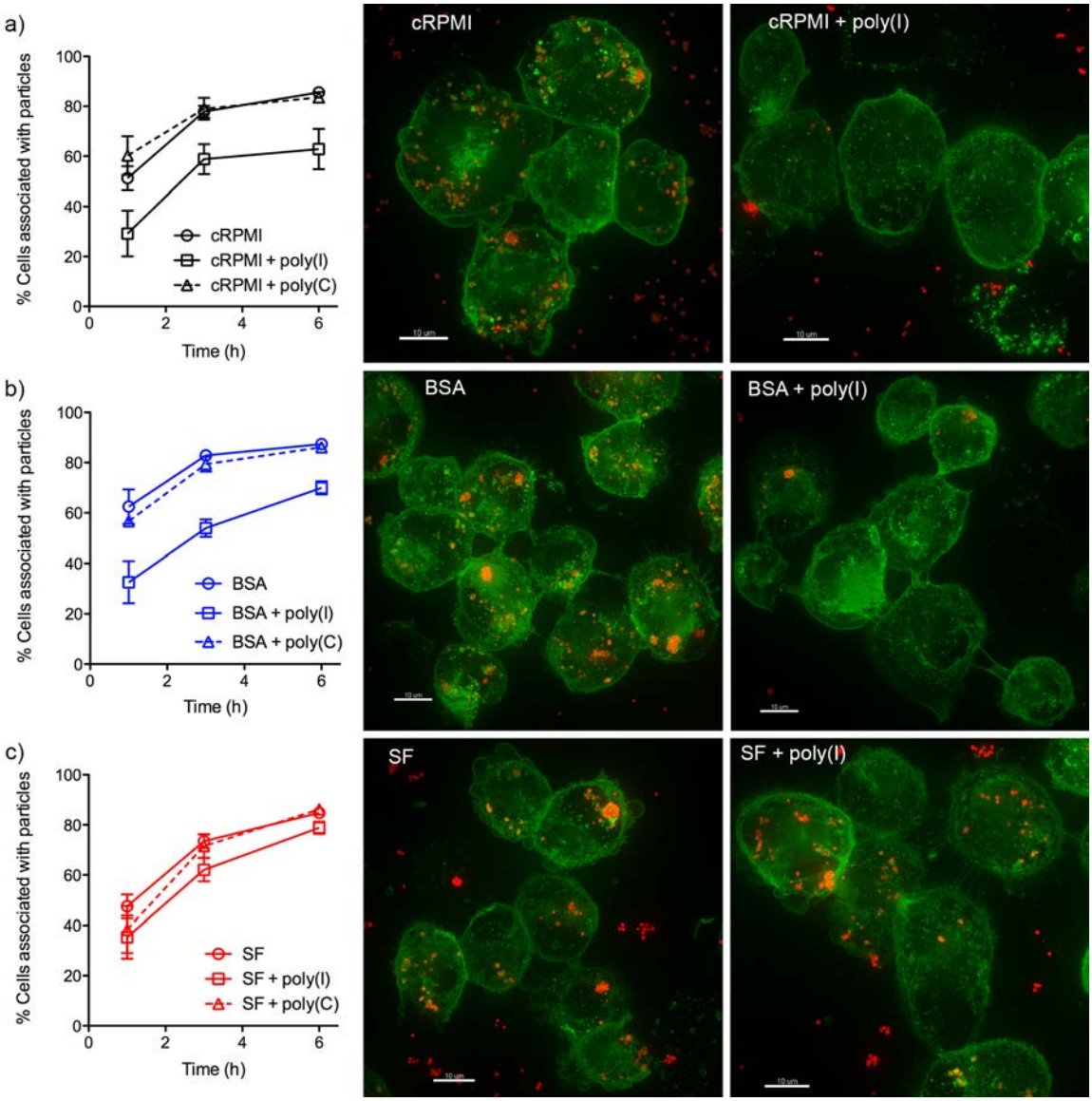

Figure 5. The role of scavenger receptor A-mediated phagocytosis in the uptake of AF633-PMA_{SH} particles in dTHP-1 cells. Cells were pretreated with poly(I) or poly(C) for 30 min prior to incubation with the particles at a particle-to-cell ratio of 100:1 in complete growth medium (cRPMI), BSA-containing medium (BSA), or serum free medium (SF) at 37 °C, 5% CO_2 for various time intervals. The percentage of cells associated with particles was measured by flow cytometry. Data are the mean ± standard error of at least three independent experiments, with at

least 10 000 cells analyzed in each experiment. The cellular uptake of the particles after 3 h incubation was visualized by fluorescence deconvolution microscopy. The maximum intensity projection images show the cell membrane (stained with AF488-wheat germ agglutinin, green) and the internalized AF633-PMA_{SH} particles (Red). Scale bars = 10 μm.

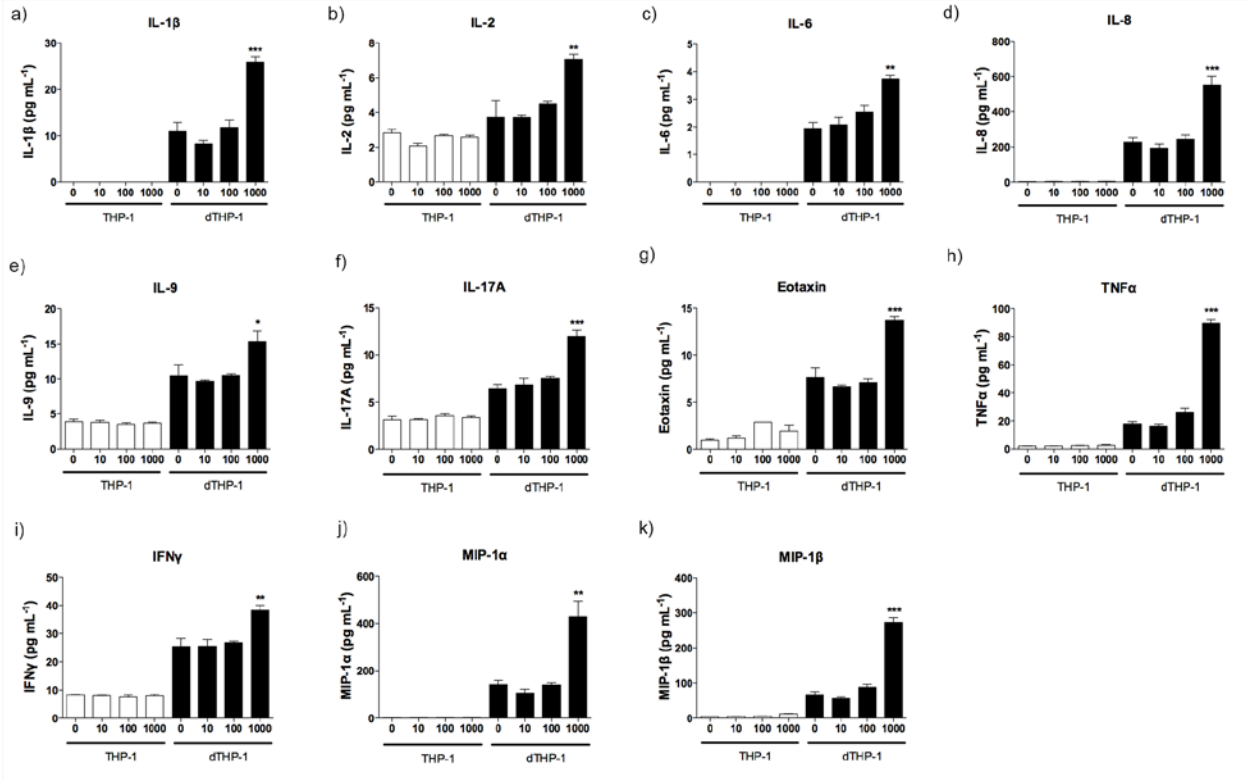

Figure 6. Pro-inflammatory cytokine secretion by THP-1 and dTHP-1. The cells were incubated with an increasing ratio of PMA_{SH} NPPs in cRPMI at 37 °C, 5% CO_2 for 24 h. The supernatant was harvested and cytokine responses were measured in triplicate. Data are expressed as mean ± standard error; $*p < 0.05$, $**p < 0.005$, $***p < 0.0001$ *versus* untreated cells (1-way ANOVA Dunnett's Multiple Comparison Test).

REFERENCES

1. Auffray, C.; Sieweke, M. H.; Geissmann, F. Blood Monocytes: Development, Heterogeneity, and Relationship with Dendritic Cells. *Annu. Rev. Immunol.* **2009**, *27*, 669-692.

2. Murray, P. J.; Wynn, T. A. Protective and Pathogenic Functions of Macrophage Subsets. *Nat. Rev. Immunol.* **2011**, *11*, 723-737.

3. Dobrovolskaia, M. A.; McNeil, S. E. Immunological Properties of Engineered Nanomaterials. *Nat. Nanotechnol.* **2007**, *2*, 469-478.

4. Albanese, A.; Tang, P. S.; Chan, W. C. The Effect of Nanoparticle Size, Shape, and Surface Chemistry on Biological Systems. *Annu. Rev. Biomed. Eng.* **2012**, *14*, 1-16.

5. Monopoli, M. P.; Aberg, C.; Salvati, A.; Dawson, K. A. Biomolecular Coronas Provide the Biological Identify of Nanosized Materials. *Nat. Nanotechnol.* **2012**, *7*, 779-786.

6. Lesniak, A.; Fenaroli, F.; Monopoli, M. P.; Aberg, C.; Dawson, K. A.; Salvati, A. Effects of the Presence or Absence of a Protein Corona on Silica Nanoparticle Uptake and Impact on Cells. *ACS Nano* **2012**, *6*, 5845-5857.

7. Lesniak, A.; Salvati, A.; Santos-Martinez, M. J.; Radomski, M. W.; Dawson, K. A.; Aberg, C. Nanoparticle Adhesion to the Cell Membrane and its Effect on Nanoparticle Uptake Efficiency. *J. Am. Chem. Soc.* **2013**, *135*, 1438-1444.

8. Lunov, O.; Syrovets, T.; Loos, C.; Beli, J.; Delacher, M.; Tron, K.; Nienhaus, G. U.; Musyanovych, A.; Mailander, V.; Landfester, K. *et al.* Differential Uptake of Functionalized Polystyrene Nanoparticles by Human Macrophages and a Monocytic Cell Line. *ACS Nano* **2011**, *5*, 1657-1669.

9. Deng, Z. J.; Liang, M.; Monteiro, M.; Toth, I.; Minchin, R. F. Nanoparticle-Induced Unfolding of Fibrinogen Promotes Mac-1 Receptor Activation and Inflammation. *Nat. Nanotechnol.* **2011**, *6*, 39-44.

10. Nel, A. E.; Madler, L.; Velegol, D.; Xia, T.; Hoek, E. M.; Somasundaran, P.; Klaessig, F.; Castranova, V.; Thompson, M. Understanding Biophysiochemcial Interactions at the Nano-Bio Interface. *Nat. Mater.* **2009**, *8*, 543-557.

11. Zhang, D.; Neumann, O.; Wang, H.; Yuwono, V. M.; Barhoumi, A.; Perham, M.; Hartgerink, J. D.; Wittung-Stafshede, P.; Halas, N. J. Gold Nanoparticles Can Induce the Formation of Protein-Based Aggregates at Physiological pH. *Nano Lett.* **2009**, *9*, 666-671.

12. Wang, Y.; Angelatos, A. S.; Caruso, F. Template Synthesis of Nanostructured Materials *via* Layer-by-Layer Assembly. *Chem. Mater.* **2008**, *20*, 848-858.

13. Wang, Y.; Price, A. D.; Caruso, F. Nanoporous Colloids: Building Blocks for a New Generation of Structured Materials. *J. Mater. Chem.* **2009**, *19*, 6451-6464.

14. Tan, J.; Wang, Y.; Yip, X.; Glynn, F.; Shepherd, R. K.; Caruso, F. Nanoporous Peptide Particles for Encapsulating and Releasing Neutrophic Factors in an Animal Model of Neutrodegeneration. *Adv. Mater.* **2012**, *24*, 3362-3366.

15. Cui, J.; De Rose, R.; Best, J. P.; Johnston, A. P. R.; Alcantara, S.; Liang, K.; Such, G. K.; Kent, S. J.; Caruso, F. Mechanically Tunable, Self-Adjuvanting Nanoengineered Polypeptide Particles. *Adv. Mater.* **2013**, *25*, 3468-3472.

16. Cui, J.; Yan. Y.; Wang, Y.; Caruso, F. Templated Assembly of pH-Labile Polymer-Drug Particles for Intracellular Drug Delivery. *Adv. Funct. Mater.* **2012**, *22*, 4718-4723.

17. Yan, Y.; Lai, Z. W.; Goode, R. J.; Cui, J.; Bacic, T.; Kamphuis, M. M. J.; Nice, E. C.; Caruso, F. Particles on the Move: Intracellular Trafficking and Asymmetric Mitotic Partitioning of Nanoporous Polymer Particles. *ACS Nano* **2013**, *7*, 5558-5567.

18. Walkey, C. D.; Chan, W. C. W. Understanding and Controlling the Interaction of Nanomaterials with Proteins in a Physiological Environment. *Chem. Soc. Rev.* **2012**, *41*, 2780-2799.

19. Tenzer, S.; Docter, D.; Kuharev, J.; Musyanovych, A.; Fetz, V.; Hecht, R.; Schlenk, F.; Fischer, D.; Kiouptsi, K.; Reinhardt, C. *et al.* Rapid Formation of Plasma Protein Corona Critically Affects Nanoparticle Pathophysiology. *Nat. Nanotechnol.* **2013**, *8*, 772-781.

20. Ishihama, Y.; Oda, Y.; Tabata, T.; Sato, T.; Nagasu, T.; Rappsilber, J.; Mann, M. Expotentially Modified Protein Abundance Index (emPAI) for Estimation of Absolute Protein Amount in Proteomics by the Number of Sequenced Peptides Per Protein. *Mol. Cell Proteomics* **2005**, *4*, 1265-1272.

21. Giles, S.; Czuprynski, C. Novel Role for Albumin in Innate Immunity: Serum Albumin Inhibits the Growth of *Blastomyces dermatitidis* Yeast Form *In Vitro*. *Infect. Immun.* **2003**, *71*, 6648-6652.

22. Monopoli, M. P.; Walczyk, D.; Campbell, A.; Elia, G.; Lynch, I.; Bombelli, F. B.; Dawson, K. A. Physical-Chemical Aspects of Protein Corona: Relevance to *In Vitro* and *In Vivo* Biological Impacts of Nanoparticles. *J. Am. Chem. Soc.* **2011**, *133*, 2525-2534.

23. Walczyk, D.; Bombelli, F. B.; Monopoli, M. P.; Lynch, I.; Dawson, K. A. What the Cell "Sees" in Bionanoscience. *J. Am. Chem. Soc.* **2010**, *132*, 5761-5768.

24. Huhn, D.; Kantner, K.; Geidel, C.; Brandholt, S.; De Cock, I.; Soenen, S. J.; Rivera-Gil, P.; Montenegro, J. M.; Braeckmans, K.; Mullen, K. *et al.* Polymer-Coated Nanoparticles Interacting with Proteins and Cells: Focusing on the Sign of the Net Charge. *ACS Nano* **2013**, *7*, 3253-3263.

25. Lacerda, S. H.; Park, J. J.; Meuse, C.; Pristinski, D.; Becker, M. L.; Karim, A.; Douglas, F. Interaction of Gold Nanoparticles with Common Human Blood Proteins. *ACS Nano* **2010**, *4*, 365-379.

26. Lassen, B.; Malsten, M. Structure of Protein Layers during Competitive Adsorption. *J. Colloid Interface Sci.* **1996**, *180*, 339-349.

27. Rabe, M.; Verdes, D.; Seeger, S. Understanding Protein Adsorption Phenomena at Solid Surfaces. *Adv. Colloid Interface Sci.* **2011**, *162*, 87-106.

28. Patel, P. C.; Giljohann, D. A.; Daniel, W. L.; Zheng, D.; Prigodich, A. E.; Mirkin, C. A. Scavenger Receptors Mediate Cellular Uptake of Polyvalent Oligonucleotide-Functionalized Gold Nanoparticles. *Bioconjug. Chem.* **2010**, *21*, 2250-2256.

29. Chang, Z. L. Recent Development of the Mononuclear Phagocyte System. *Biol. Chem.* **2009**, *101*, 709-721.

30. Daigneault, M.; Preston, J. A.; Marriott, H. M.; Whyte, M. K. B.; Dockrell, D. H. The Identification of Markers of Macrophage Differentiation in PMA-Stimulated THP-1 Cells and Monocyte-Derived Macrophages. *PLos One* **2010**, *5*, e8668.

31. Maess, M. B.; Sendelbach, S.; Lorkowski, S. Selection of Reliable Reference Genes During THP-1 Monocyte Differentiation into Macrophages. *BMC Mol. Biol.* **2010**, *11*, 90.

32. Chen, X.-W.; Shen, Y.; Sun, C.-Y.; Wu, F.-X.; Chen, Y.; Yang, C.-D. Anti-Class A Scavenger Receptor Autoantibodies from Systems Lupus Erythematosus Patients Impair Phagocytic Clearance of Apoptotic Cells by Macrophages *In Vitro*. *Arthritis Res. Ther.* **2011**, *13*, R9.

33. Platt, N.; Gordon, S. Scavenger Receptors: Diverse Activities and Promiscuous Binding of Polyanionic Ligands. *Chem. Biol.* **1998**, *5*, R193-203.

34. Pluddemann, A.; Neyen, C.; Gordon, S.; Peiser, L. A Sensitive Solid-Phase Assay for identification of Class A Macrophage Scavenger Receptor Ligands Using Cell Lysate. *J. Immunol. Methods* **2008**, *329*, 167-175.

35. Martinez, V. G.; Moestrup, S. K.; Holmskov, U.; Mollenhauer, J.; Lozano, F. The Conserved Scavenger Receptor Cysteine-Rich Superfamily in Therapy and Diagnosis. *Pharmacol. Rev.* **2011**, *63*, 967-1000.

36. de Winther, M. P.; van Dijk, K. W.; Havekes, L. M.; Hofker, M. H. Macrophage Scavenger Receptor Class A: A Multifunctional Receptor in Atherosclerosis. *Arterioscler. Thromb. Vasc. Biol.* **2000**, *20*, 290-297.

37. Miyata, R.; van Eeden, S. F. The Innate and Adaptive Immune Response Induced by Alveolar Macrophages Exposed to Ambient Particulate Matter. *Toxicol. Appl. Pharmacol.* **2011**, *257*, 209-226.

38. Maderna, P.; Godson, C. Phagocytosis of Apoptotic Cells and the Resolution of Inflammation. *Biochim. Biophys. Acta* **2003**, *1639*, 141-151.

39. Shapero, K.; Fenaroli, F.; Lynch, I.; Cottell, D. C.; Salvati, A.; Dawson, K. A. Time and Space Resolved Uptake Study of Silica Nanoparticles by Human Cells. *Mol. Biosyst.* **2011**, *7*, 371-378.

TOC

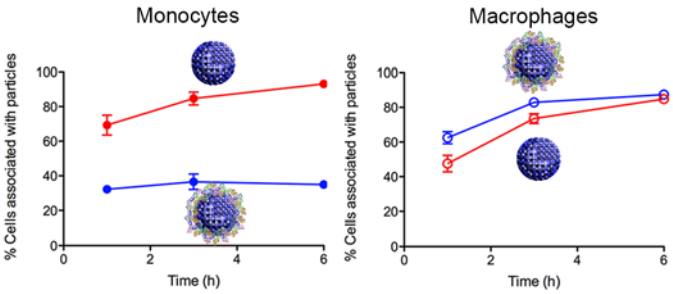
Monocytes
Macrophages
% Cells associated with particles
Time (h)
0
20
40
60
80
100
2
4
6